Slov Vet Res 2018; 55 (Suppl 20): 95–102
DOI 10.26873/SVR-634-2018

Original Research Article

UPREGULATION OF miR-155 IMPAIRS WHITE MATTER SPARING AT THE INJURY AREA FOLLOWING CONTUSIVE SPINAL CORD INJURY IN MICE

Hayam A. Hussein[1], Mohamed Gomaa[1]*, Rochelle J. Deibert[2,3], Lesley C. Fisher[2,3], Stephanie A. Amici[2], Mireia Guerau-de-Arellano[2], Michele D. Basso[2], Ahmed E. Behery[1]

[1]Surgery, Anesthesiology and Radiology Department, Faculty of Veterinary Medicine, Zagazig University, 44511, Egypt, [2]School of Health and Rehabilitation Sciences, [3]Center for Brain and Spinal Cord Repair, the Ohio State University, Columbus, OH 43210 USA

*Corresponding author, E-mail: gomaasurgeon@yahoo.com

Abstract: This study was conducted to characterize the effect of miR-155 overexpression on white matter sparing and lesion size following contusion injury of spinal cord in mice. 60 C57BL/6J wild-type and 60 B6.Cg miR-155 knockout mice were used to induce moderate to severe contusive spinal cord injury at T9 segment. All used mice were female, 8–20 weeks old and weighing 18^{+} gm. Mice were divided into two main groups; for Real-time reverse transcriptase polymerase chain reaction (RT-PCR) and histology, then subdivided into five subgroups; 1, 3, 7, 14 and 42 days after the contusion according to time point, each was compared to naive control group. Fresh and fixed tissue were taken from thoracic segments (lesion area) from all time points, dissected and then evaluated using RT-PCR and histology (Eriochrome stain), respectively. We identified significant upregulation of miR-155 at the lesion site by 3 days and continued up to 6 weeks after the injury. Following spinal cord injury, the miR-155 overexpression was accompanied with severe cord damage and less tissue repair while more white matter sparing and smaller lesion size were detected in miR-155 knockout group.

Key words: miR-155; spinal cord injury; sontusion; spicenter; shite matter sparing

Introduction

Traumatic spinal cord injury (SCI) is characterized by primary or acute (seconds to minutes following SCI), secondary (minutes to weeks following SCI), and chronic (months to years following SCI) deterioration phases (1,2). The primary insult to the epicenter area damages spinal cord tissues, ruptures blood vessels, opens the blood-spinal cord barrier (BSCB), and causes edema (3,4). However, secondary events are mainly induced in response to pro-apoptotic signals and severe immune reaction through inflammatory cell trafficking, activation of resident CNS cells, and expression of pro-inflammatory mediators causing neurotoxicity and tissue damage, mainly close to the injury epicenter, and then extends at both directions; rostral and caudal to the injury site. Apoptosis predominately occurs at oligodendroglia, microglia and neurons (5-10).

Micro RNA (miR-155) is a non-coding, short (about 20 nucleotides) and single-stranded RNAs. miR-155 is a negative regulator for specific genes by either impairing

Received: August 2018
Accepted for publication: September 2018

their translation into protein or inducing mRNA disintegration. A small sequence in the 3′-untranslated region (3′-UTR) of a specific gene is a target area for miR-155 (11-13). miR-155 is involved in the secondary pathogenesis following SCI through controlling inflammation, BSCB permeability, apoptosis and axonal sprouting (14,15). miR-155 plays a major role in axon dieback via downregulating growth-promoting protein and provoking growth inhibitory conditions after SCI. Moreover, genetic ablation of miR-155 enhances axon sprouting and increases neuronal functionality following SCI (14).

Interestingly, miR-155 is one of the highly expressed miRs in various inflammation-related neurological disorders of the brain or spinal cord such as traumatic injury, stroke, multiple sclerosis, amylotrophic lateral sclerosis, encephalomyelitis, and Alzheimer's disease (14,16-20).

miR-155 contributes to the immune effects elicited by blood borne-monocytes, migrated macrophages and microglial cells in CNS. miR-155 mediates hippocampal-associated neuroinflammatory response via microglial activation and IL6 expression. Additionally, microglial miR-155 up-regulation enhances neural stem cells (NSCs) astrogliogenesis (19). On the other hand, miR-155 increases the expression of inflammatory signaling molecules and activates the inflammatory macrophage subtype through upregulating its target genes (e.g. Nos2, Il-1b and Tnfa) and protein in addition to oxidative metabolite production (15,16,18,21-23).

Therefore this study was performed to characterize the effect of miR-155 upregulation on white matter repair after induction of contusive spinal cord injury in mice.

Material and methods

Mice

All animal experiments were conducted in accordance with protocols approved by the Ohio State University Institutional Laboratory Animal Care and Use Committee. Two mice strains including 60 C57BL/6J wild-type (WT) and 60 B6.Cg miR-155 knockout (KO) mice were obtained from Jackson Laboratories. These animals were 120 female, 8–20 weeks old and weighing 18^{+} gm. Mice were randomly allocated into two main groups; group I: for PCR and group II: for histology purposes (each group contains 60 mice: 30 from each strain). Each group was subdivided into naïve control subgroup and five subgroups according to time point; 1d, 3d, 7d, 14d and 42d groups (5 mice at each subgroup). Group division was illustrated in Table (1). Mice were housed 3–5 per cage and provided standard food and filtered tap water *ad libitum*.

Table 1: Distribution of 120 mice used in investigation of the effect of miR-155 upregulation on white matter repair after induction of contusive spinal cord injury in mice

Time points	PCR groups		Histology groups	
	Naive control *(n=10)	SCI (n=50)	Naive control (n=10)	SCI (n=50)
1 dpi	5WT, 5miR-155KO mice as control for whole PCR experiments	5WT, 5KO	5WT, 5miR-155KO mice as control for whole histology experiments	5WT, 5KO
3 dpi		5WT, 5KO		5WT, 5KO
7 dpi		5WT, 5KO		5WT, 5KO
14 dpi		5WT, 5KO		5WT, 5KO
42 dpi		5WT, 5KO		5WT, 5KO

*n: total number in each subgroup, SCI: Spinal Cord Injury, WT: Wild-Type, KO: Knockout

Surgical procedures

Spinal cord injury was conducted as previously described by Hansen et al. (9). Mice were generally anesthetized with a ketamine (138 mg/kg body weight) and xylazine (20 mg/kg body weight) cocktail (intraperitoneally-injected) and given prophylactic antibiotics gentamycin (gentocin®, 1 mg/kg, S.C.). Aseptic preparation to the site of injury (at the

dorsal aspect 1-2 cm from the point of shoulder) then putting the animal on stable heating pad (34˚), putting gauze pad under thorax to raise animal and decrease pressure on respiratory muscles during clamping then start surgery under the microscope (Leica MZ8). A ninth thoracic vertebra (T9) laminectomy was performed to expose the dura. After stabilizing the spinous processes of T8 and T10, a moderately severe contusion injury was induced by 75 kilodynes of force using the Infinite Horizon (IH) device. Biomechanics of the injury were monitored on day 0. The incision was closed in standard manner and 2 ml of sterile saline was given subcutaneously. The mice from both genotypes were distributed randomly into two main groups and each group was subdivided into five subgroups.

Postoperative care

During recovery, mice were covered with a warm towel and positioned on a warm heating pad, received antibiotics (1 mg/kg gentocin, S.C.) and subcutaneous injection of saline (2, 2, 1, 1, and 1 ml) for the 5 successive days post injury (dpi). Bladders were manually voided twice daily. They were housed in a temperature controlled room at 37°C for 24h. Food and water were provided *ad libitum*.

Tissue collection in PCR groups

Mice deeply anesthetized and transcardially perfused with 0.1 M phosphate buffered saline (PBS; pH 7.4) at naive, 1d, 3d, 7d, 14d or 42d after SCI. Tissue from injury area was obtained as soon as possible to limit potential degradation of biomarkers in tissue samples. Tissue was placed in Eppendorf tube and then samples were flash frozen into liquid nitrogen. Once frozen, the vial was removed from the liquid nitrogen and stored at –80°C (23).

RNA Isolation

To examine RNA expression at WT samples, cellular RNA was isolated using the miRVana kit (Life Technologies) according to manufacturer specifications. RNA quality/ concentration was quantified using a Nanodrop spectrophotometer (ThermoScientific, Wilmington, DE). Extracted RNA was stored at -80°C until analysis (23).

Real-Time reverse transcriptase PCR

miRNA expression was determined by Taqman Real-Time PCR using miR-155 and sno-202 primer and probe sets (Applied biosystems). TaqMan® Catalog number: 4427975. Assay ID: MI0000177. Gene Symbol: miR-155. Gene sequence: UUAAUGCUAAUUGUGAUAGGGGU. Briefly, after an initial cDNA transcription using specific miRNA primers to generate cDNA using 10 ng RNA as a template, PCR was performed using Taqman universal PCR mix and gene-specific miRNA primers and probe mixture (TaqMan microRNA reverse transcription kit (Applied Biosystems). Reaction mixture was run in an Applied Biosystems 7900 Real-Time PCR machine with denaturation step at 95°C for 10 minutes, followed by 40 cycles of denaturation at 95°C for 15 seconds and primer annealing/extension at 60°C for 60 seconds. miRNA expression was normalized to the small RNA sno202 (23).

Histopathological evaluation

Mice deeply anesthetized and intracardially perfused with 0.1 M phosphate buffered saline (PBS; pH 7.4) followed by 4% paraformaldehyde (pH 7.2) at naïve, 1d, 3d,7d, 14d or 42d after SCI. Spinal cord segments from injury epicenter were post-fixed for 1h in 4% paraformaldehyde, rinsed overnight in 0.2M phosphate buffer (PB, pH 7.4) then cryoprotected in 30% sucrose before being embedded in Optimal Cutting Temperature compound OCT (Thermoscientific) and frozen on dry ice (9).

White Matter Sparing (WMS)

Thoracic tissues were collected from the sites of SCI from naives, 1d, 3d, 7d, 14d and 42d groups and transversely cut 20 um thick on a Microm HM505E cryostat. Using immuno-histochemical procedure, the tissues were stained with eriochrome cyanine (EC) to identify the white matter spared of the lesion epicenter. In addition to EC, a 5% iron aluminum and borax ferricyanide cocktail were

used. Light microscopy measures were used to evaluate the tissue, and tissue images were converted to computer images (MCID-Elite, Imaging Research, Ontario). Using a Cavalerri estimator (In stereology program), a grid was positioned over the tissue at random, and each point within the grid was designated as white matter or grey matter. Per each image area, point totals were combined and calculated to area as follows: estimated area = (ΣP) * (a/p), where ΣP is the total point per section and a/p is the total area per point. Average white matter spared and lesion area was compared between groups to identify differences (9, 24).

Statistical analyses

Group differences for white matter sparing (WMS) were compared using Two-way analysis of variance (ANOVA) with a Tukey's post-hoc analysis. The null hypothesis was rejected at the $p \leq 0.05$ level. All statistical analyses utilized the IBM SPSS program, SPSS Inc. Mean and standard error of the mean (SE) were shown throughout (9).

Results

miR-155 overexpression at the injury epicenter following SCI

Using Taqman RT-PCR, we found significant increase in miR-155 expression at the injured WT epicenter compared to naive WT samples (Relative fold expression=1) starting at 3 dpi and remained upregulated up to 42 dpi following contusion injury. miR155 upregulated at 3 dpi (Relative fold expression=3.4), 7dpi (Relative fold expression=3.8), 14d (Relative fold expression=3.2) and highly overexpressed at 42 dpi (Relative fold expression=4.5) (p=0.001) as shown in Figure (1).

White matter sparing (WMS) is directly affected by miR-155 elevation after SCI

Upregulation of miR-155 after SCI at the lesion area enhances the injury severity and impairs the spinal cord repair after SCI.

White matter sparing at the injured cord, was highly suppressed in WT mice compared to miR-155 KO mice especially at 7dpi (Figure 2). In addition, injury area in WT mice was larger than in miR-155KO mice across the lesion epicenter (Figure 3), indicating that miR-155 deletion enhances tissue repair. Eriochrome stain was used to identify intact myelin in the white matter. Well-differentiated white matter and grey matter were detected at sections of uninjured control. Injured sections from both strains and at all time points were stained with Eriochrome stain to show lesion size and degree of tissue repair following SCI (Figure 4).

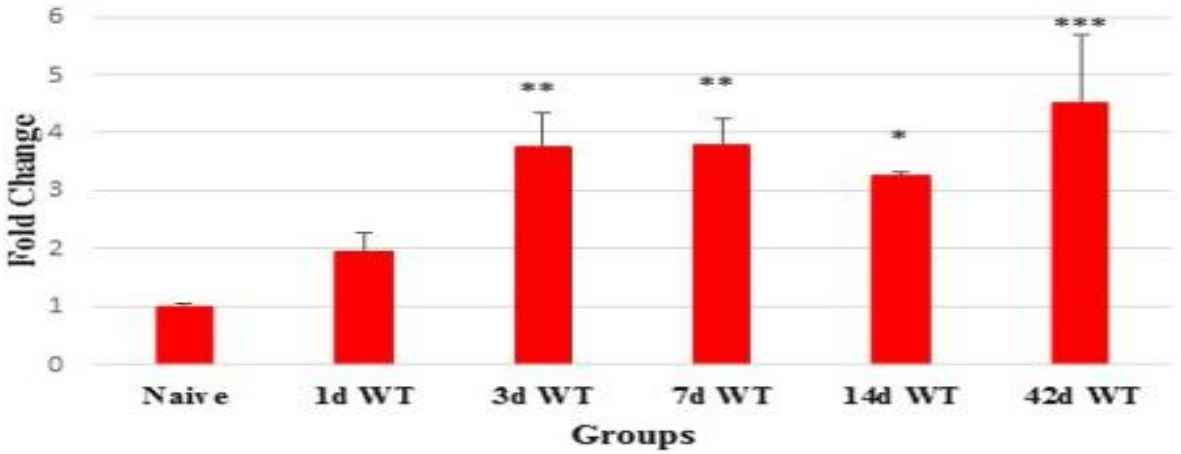

Figure 1: miR-155 upregulation at Injury Epicenter using RT-PCR technique. Contusive spinal cord injury (SCI) upregulates miR-155 at the lesion epicenter of wild-type (WT) mice up to six weeks, compared with WT naive control mice. Means with (*) are significantly different than naïve controls

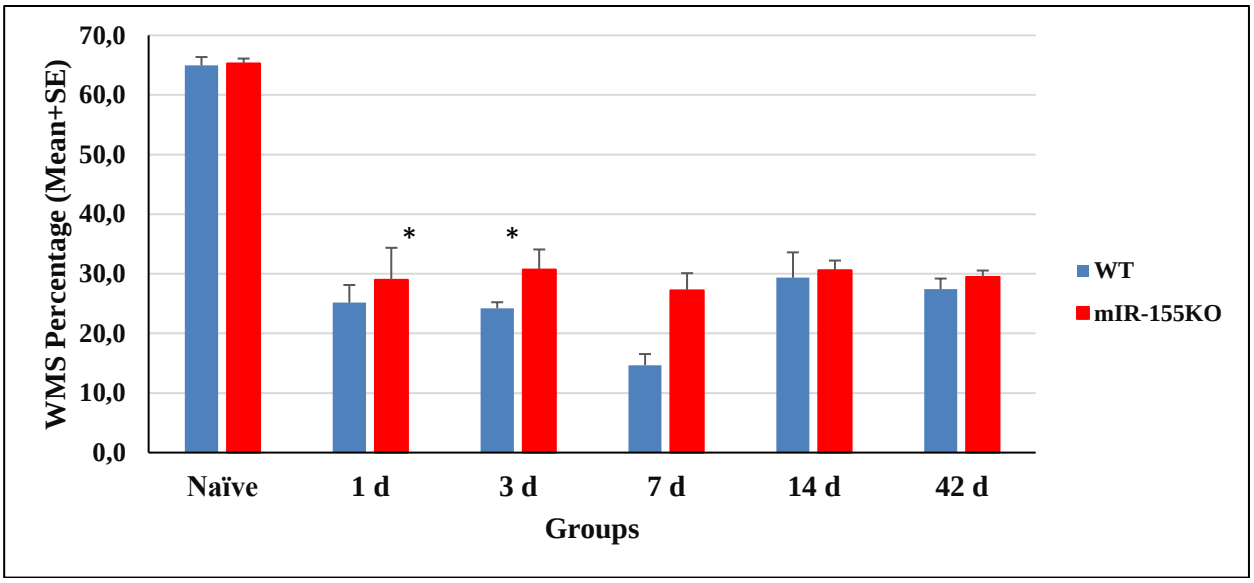

Figure 2: Total WMS Percentage across groups after spinal cord injury (SCI). miR-155 knockout (KO) mice showed more protected white matter than wild-type (WT) control mice at the injury site following SCI. Means of white matter sparing percentage with (*) are significantly different than naïve controls

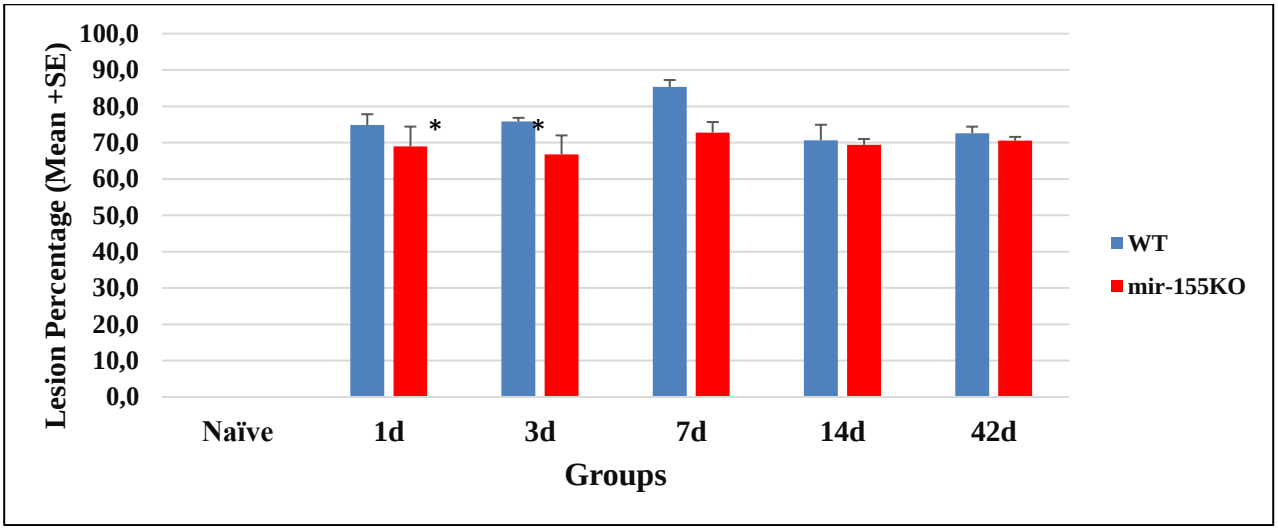

Figure 3: Spinal cord lesion epicenter percentage across groups after spinal cord injury (SCI). WT mice has larger lesion size than miR-155 knockout (KO) mice at the lesion epicenter after SCI. Means with (*) are significantly different than naïve controls

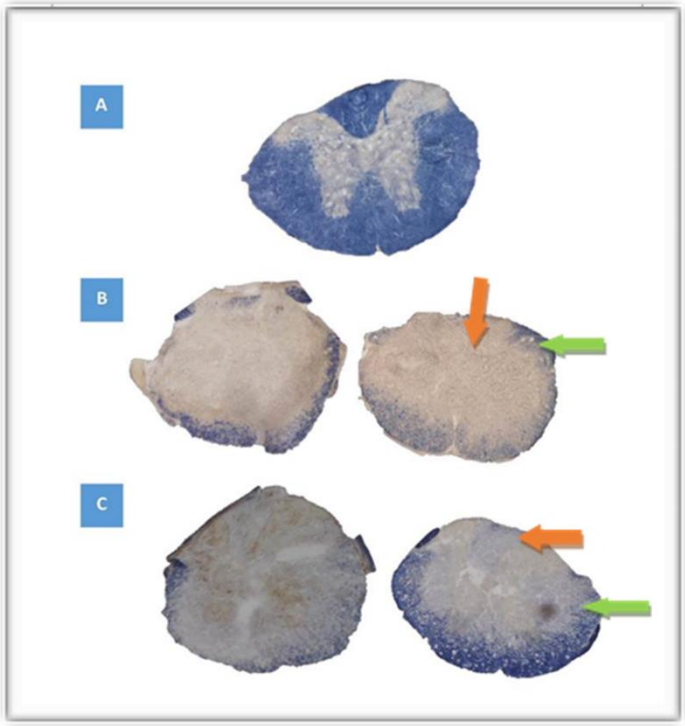

Figure 4: Eriochrome Staining showing the lesion area and degree of tissue repair after spinal cord injury (SCI). Eriochrome was used to identify intact myelin in white matter (bluish colored). A: stained section for naive control mouse showed well-differentiated white and gray matter. B at 3dpi, C at 7dpi: miR-155 knockout (KO) mice (Right side images) had significantly smaller lesions (orange arrow) and more preserved white matter (green arrow) than wild-type (WT) lesions (Left side images) with notable changes evident at injury epicenter. Colored outlines represent lesion size in every animal examined for each genotype at epicenter

Discussion

At the present study, significant overexpression of miR-155 was detected at the injury epicenter starting at 3 dpi and continued high up to 6 weeks following spinal contusion injury. This finding is in agreement with Gaudet et al. (14). miR-155 is markedly produced by microglia (19,22) and macrophages (14). Moreover, inflammatory molecules produced by immune cells stimulate miR-155 overexpression (25,26). Elevated miR-155 upregulates pro-inflammatory signaling while downregulates anti-inflammatory molecules (27,28), which results in activation of inflammatory macrophages. In the CNS, miR-155 is implicated in the pathogenesis of SCI, stroke, multiple sclerosis, amylotrophic lateral sclerosis, encephalomyelitis and Alzheimer's disease (14-17,29,30).

We revealed a novel role for miR-155 in SCI repair and pathology. miR-155 KO spinal cords had reduced lesion size and improved white matter sparing. Prominent neuronal loss is marked by 8 hr post injury in rat SCI, beginning at the gray matter and then extend to the white matter. While apoptosis of glial cells is most distinct by 24 hr post injury, and then peaked again by 7 dpi particularly in the white matter (5). Inflammatory cascade induced post-injury is implicated in the tissue deterioration and loss of spinal cord functionality. Activated macrophages /microglia are primary contributors to secondary pathogenesis after SCI through expression of toxic molecules such as TNF-α, IL-1β, IL-6, nicotinamide adenine dinucleotide phosphate (NADPH) oxidases, inducible nitric oxide synthase (iNOS), nitric oxide (NO), reactive oxygen species (ROS) and matrix metalloproteinases (MMPs) which initiate neuroinflammatory reactions at the injury site and induce tissue damage through activation of

astrocytes, loss of oligodendrocytes and neurons, in addition to demyelination (31-33). Caspases, specifically caspase-3, 8, 9 and 10, are good indicators for onset of apoptosis (7, 34-37). Apoptosis can be partially restricted via miR-155-induced suppression of caspase-3 expression in activated macrophages (38). Therefore, the continued upregulation of miR-155 at the lesion area could cause more tissue pathology through promoting the toxic microenvironment.

Conclusion

It could be concluded that miR-155 deletion improved tissue repair by suppressing neuroinflammation and decreasing the secondary damage after the contusion injury.

Conflict of interest

None of the authors have any conflict of interest to declare.

Acknowledgement

The authors thank Zagazig University Egypt and Neuroscience research program and Center for brain and spinal cord injury at Ohio State University USA for funding this work.

References

1. Oyinbo C A. Secondary injury mechanisms in traumatic spinal cord injury: a nugget of this multiply cascade. Acta Neurobiol Exp (Wars) 2011; 71: 281–99.

2. Zhou X, He X, Ren Y. Function of microglia and macrophages in secondary damage after spinal cord injury. Neural Regen Res 2014; 9: 1787–95.

3. Schwab ME, Bartholdi D. Degeneration and regeneration of axons in the lesioned spinal cord. Physiol Rev 1996; 76: 319–70.

4. Beattie MS, Li Q, Bresnahan, JC. Cell death and plasticity after experimental spinal cord injury. Prog Brain Res 2000; 128: 9–21.

5. Liu XZ, Xu XM, Hu R, Du C, Zhang SX, McDonald JW, Dong HX, Wu YJ, Fan GS, Jacquin MF, Hsu CY, Choi DW. Neuronal and glial apoptosis after traumatic spinal cord injury. J Neuosci 1997; 17: 5395–406.

6. Shuman SL, Bresnahan JC, Beattie MS. Apoptosis of microglia and oligodendrocytes after spinal cord injury in rats. J Neurosci Res 1997; 50: 798–808.

7. Casha S, Yu WR, Fehlings MG. Oligodendroglial apoptosis occurs along degenerating axons and is associated with Fas and p75 expression following spinal cord injury in the rat. Neuroscience 2001; 103: 203–18.

8. Fleming JC, Norenberg MD, Ramsay DA, Dekaban GA, Marcillo AE, Saenz AD, Pasquale-Styles M, Dietrich WD, Weaver LC. The cellular inflammatory response in human spinal cords after injury. Brain 2006; 129: 3249–69.

9. Hansen CN, Fisher LC, Deibert RJ, Jakeman LB, Zhang H, Noble-Haeusslein L, White S, Basso MD. Elevated MMP-9 in the lumbar cord early after thoracic spinal cord injury impedes motor relearning in mice. The Journal of Neuroscience 2013; 33: 13101–11.

10. Hansen CN, Norden, DM, Faw TD, Deibert R, Wohleb ES, Sheridan JF, Godbout JP, Basso DM. Lumbar myeloid cell trafficking into locomotor networks after thoracic spinal cord injury. Experimental Neurology 2016; 282: 86–98.

11. Ambros V. The functions of animal microRNAs. Nature 2004; 431: 350–5.

12. Lund E, Güttinger S, Calado A, Dahlberg JE, Kutay U. Nuclear export of microRNA precursors. Science 2004; 303: 95–9.

13. Bartel DP. MicroRNAs: target recognition and regulatory functions. Cell 2009; 136: 215–33.

14. Gaudet AD, Mandrekar-Colucci S, Hall JC, Sweet DR, Schmitt PJ, Xu X, Guan Z, Mo X, Guerau-de-Arellano M, Popovich PG. miR-155 deletion in mice overcomes neuron-intrinsic and neuron-extrinsic barriers to spinal cord repair. J Neurosci 2016; 36: 8516–32.

15. Caballero-Garrido E, Pena-Philippides JC, Lordkipanidze T, Bragin D, Yang Y, Erhardt EB, Roitbak T. In vivo inhibition of miR-155 promotes recovery after experimental mouse stroke. J Neurosci 2015; 35: 12446–64.

16. Murugaiyan G, Beynon V, Mittal A, Joller N, Weiner HL. Silencing microRNA- 155 ameliorates experimental autoimmune encephalomyelitis. J. Immunol 2011; 187: 2213–21.

17. Moore CS, Rao VT, Durafourt BA, Bedell BJ, Ludwin SK, Bar-Or A, Antel JP. miR-155 as a multiple sclerosis-relevant regulator of myeloid cell polarization. Ann. Neurol 2013; 74: 709–20.

18. Guedes JR, Custodia CM, Silva RJ, de Almeida LP, Pedroso de Lima, MC, Cardoso AL. Early miR-155 upregulation contributes to neuroinflammation in Alzheimer's disease triple

transgenic mouse model. Hum Mol Genet 2014; 23: 6286-301.

19. Woodbury ME, Freilich RW, Cheng CJ, Asai H, Ikezu S, Boucher JD, Slack F, Ikezu T. miR-155 Is Essential for Inflammation-Induced Hippocampal Neurogenic Dysfunction. J Neurosci 2015; 35(26): 9764–81.

20. Yi J, Wang D, Niu X, Hu J, Zhou Y, Li Z. MicroRNA-155 deficiency suppresses Th17 cell differentiation and improves locomotor recovery after spinal cord injury. Scand J Immunol 2015; 81: 284–90.

21. Lopez-Ramirez MA, Wu D, Pryce G, Simpson JE, Reijerkerk A, King-Robson J, Kay O, de Vries H.E, Hirst MC, Sharrack B, Baker D, Male DK, Michael GJ Romero IA. MicroRNA-155 negatively affects blood–brain barrier function during neuroinflammation. FASEB J 2014; 28: 2551–65.

22. Cardoso FL, Kittel A, Veszelka S, Palmela I, Tóth A, Brites D, Deli MA, Brito M.A. Exposure to lipopolysaccharide and/or unconjugated bilirubin impair the integrity and function of brain microvascular endothelial cells. PLoS ONE 2012; 7: e35919.

23. Jablonski KA, Gaudet AD, Amici SA, Popovich PG, Guerau-de-Arellano M. Control of the inflammatory macrophage transcriptional signature by miR-155. PLoS One 2016; 11: e0159724.

24. Rabchevsky AG, Fugaccia I, Sullivan PG, Scheff SW. Cyclosporin A treatment following spinal cord injury to the rat: behavioral effects and stereological assessment of tissue sparing. J Neurotrauma 2001; 18: 513–22.

25. Ceppi M, Pereira PM, Dunand-Sauthier I, Barras E, Reith W, Santos MA, Pierre P. MicroRNA-155 modulates the interleukin-1 signaling pathway in activated human monocyte-derived dendritic cells. Proc Natl Acad Sci USA 2009; 106: 2735–40.

26. Cremer TJ, Ravneberg DH, Clay CD, Piper-Hunter MG, Marsh CB, Elton TS, Gunn, JS, Amer A, Kanneganti TD, Schlesinger LS, Butchar JP, Tridandapani S. miR-155 induction by F. novicida but not the virulent F. tularensis results in SHIP down-regulation and enhanced pro-inflammatory cytokine response. PLoS One 2009; 4: e8508.

27. Martinez-Nunez RT, Louafi F, Sanchez-Elsner T. The interleukin 13 (IL-13) pathway in human macrophages is modulated by microRNA-155 via direct targeting of interleukin 13 receptor alpha1 (IL13Ralpha1). J Biol Chem 2011; 286: 1786–94.

28. Wang P, Hou J, Lin L, Wang C, Liu X, Li D, Ma F, Wang Z, Cao X. Inducible microRNA-155 feedback promotes type I IFN signaling in antiviral innate immunity by targeting suppressor of cytokine signaling 1. J Immunol 2010; 185: 6226–33.

29. Koval ED, Shaner C, Zhang P, du Maine X, Fischer K, Tay J, Chau BN, Wu GF, Miller TM. Method for widespread microRNA-155 inhibition prolongs survival in ALS-model mice. Hum Mol Genet 2013; 22: 4127–35.

30. O'Connell RM, Taganov KD, Boldin MP, Cheng G, Baltimore D. MicroRNA-155 is induced during the macrophage inflammatory response. Proc Natl Acad Sci USA 2007; 104: 1604–9.

31. Zhou X, He X, Ren Y. Function of microglia and macrophages in secondary damage after spinal cord injury. Neural Regen Res 2014; 9: 1787–95.

32. Noble LJ, Donovan F, Igarashi T, Goosed S, Werb Z. Matrix metalloproteinases limit functional recovery after spinal cord injury by modulation of early vascular events. J Neurosci 2002; 22: 7526–35.

33. Pajoohesh-Ganji A, Byrnes KR. Novel neuroinflammatory targets in the chronically injured spinal cord. Neurotherapeutics 2011; 8: 195–205.

34. Baker SJ, Reddy EP. Modulation of life and death by the TNF receptor superfamily. Oncogene 1998; 17: 3261–70.

35. Emery E, Aldana P, Bunge MB, Puckett W, Srinivasan A, Keane RW, Bethea J, Levi AD. Apoptosis after traumatic human spinal cord injury. J Neurosurg 1998; 89: 911–20.

36. Lee YB, Yune TY, Baik SY, Shin YH, Du S, Rhim H, Lee EB, Kim YC, Shin ML, Markelonis GJ, Oh TH. Role of tumor necrosis factor-a in neuronal and glial apoptosis after spinal cord injury. Exp Neurol 2000; 166: 190–5.

37. Li M, Ona VO, Chen M, Kaul M, Tenneti L, Zhang X, Stieg PE, Lipton SA, Friedlander RM. Functional role and therapeutic implications of neuronal caspase-1 and -3 in a mouse model of traumatic spinal cord injury. Neuroscience 2000; 99: 333–42.

38. De Santis R, Liepelt A, Mossanen JC, Dueck A, Simons N, Mohs A, Trautwein C, Meister G, Marx G, Ostareck-Lederer, A, Ostareck DH. miR-155 targets Caspase-3 mRNA in activated macrophages. RNA Biol 2016; 13: 43–58.